

Free energy of cluster formation and a new scaling relation for the nucleation rate

Kyoko K. Tanaka,¹ Jürg Diemand,² Raymond Angéllil,² and Hidekazu Tanaka¹

¹*Institute of Low Temperature Science, Hokkaido University, Sapporo 060-0819, Japan*

²*Institute for Computational Science, University of Zürich, 8057 Zürich, Switzerland*

(Dated: 16 January 2022)

Recent very large molecular dynamics simulations of homogeneous nucleation with $(1-8) \cdot 10^9$ Lennard-Jones atoms [Diemand et al. *J. Chem. Phys.* **139**, 074309 (2013)] allow us to accurately determine the formation free energy of clusters over a wide range of cluster sizes. This is now possible because such large simulations allow for very precise measurements of the cluster size distribution in the steady state nucleation regime. The peaks of the free energy curves give critical cluster sizes, which agree well with independent estimates based on the nucleation theorem. Using these results, we derive an analytical formula and a new scaling relation for nucleation rates: $\ln J'/\eta$ is scaled by $\ln S/\eta$, where the supersaturation ratio is S , η is the dimensionless surface energy, and J' is a dimensionless nucleation rate. This relation can be derived using the free energy of cluster formation at equilibrium which corresponds to the surface energy required to form the vapor-liquid interface. At low temperatures (below the triple point), we find that the surface energy divided by that of the classical nucleation theory does not depend on temperature, which leads to the scaling relation and implies a constant, positive Tolman length equal to half of the mean inter-particle separation in the liquid phase.

PACS numbers: 05.10.-a, 05.70.Np, 05.70.Fh, 64.60.Qb

Keywords: molecular dynamics simulation, nucleation, phase transitions, scaling relation

I. INTRODUCTION

The nucleation process of supersaturated vapors into liquids (or solids) has been studied for a long time, however, there is still a serious gap in our understanding. The classical nucleation theory (CNT)¹⁻³ is a very widely used model for describing nucleation and provides the nucleation rates as a function of temperature, supersaturation ratio, and macroscopic surface tension of a condensed phase. However, several studies have found that the CNT fails to explain the nucleation rates observed in experiments⁴⁻¹⁵. For example, the error is the order of 10^{11-20} for argon^{14,15}. In addition to laboratory experiments, numerical simulations of molecular dynamics (MD) or Monte Carlo (MC) simulations showed that the nucleation rates obtained by numerical simulations are significantly different from predictions by the CNT¹⁶⁻³⁸. Until now several modifications to the CNT were proposed. It was also noted that several nucleation rate data sets exhibited empirical temperature scalings³⁹⁻⁴². Although there have been significant advances in the theoretical models, a quantitatively reliable theoretical model does not yet exist.

Recently, Diemand et al.³⁷ presented large-scale molecular dynamics (MD) simulations of homogeneous vapor-to-liquid nucleation of $(1-8) \times 10^9$ Lennard-Jones atoms, covering up to $1.2 \mu\text{s}$ (5.6×10^7 steps). The simulations cover a wide range of temperatures and supersaturation ratios. This study measured various quantities such as nucleation rates, critical cluster sizes, and sticking probabilities of vapor molecules, and it was successful in quantitatively reproducing argon nucleation rates at the same pressures, supersaturations and temperatures as in the

SSN (Supersonic Nozzle Nucleation) argon experiment¹⁵. Here we use these MD results to determine the free energies of cluster formation (Sec. III) and their scaling (Sec. IV), which is expected to be of use in the construction of a high-precision nucleation model.

II. EMPIRICAL SCALING RELATIONS

Hale and Thomason⁴² suggested that the nucleation rate J obtained by MC simulations using LJ molecules was scaled by $\ln S/(T_c/T - 1)^{1.5}$ over a range of $J = (10^4 - 10^7)\text{cm}^{-3} \text{ s}^{-1}$ which corresponds to $(10^{-30} - 10^{-27})\sigma^{-3}\tau^{-1}$, where T , T_c , σ , and τ are the temperature, critical temperature, a parameter of length ($= 3.405 \text{ \AA}$), and a time unit ($= 2.16 \text{ ps}$). Figure 1 shows that nucleation rates obtained by the MD and MC simulations for LJ molecules and experimental results for argon as a function of $\ln S/(T_c/T - 1)^{1.5}$ and $\ln S/(T_c/T - 1)^{1.3}$. The scaling by $\ln S/(T_c/T - 1)^{1.5}$ works for MC simulations over a limited range, however, the nucleation rates obtained by all MD simulations and some experiments are rather scaled by $\ln S/(T_c/T - 1)^{1.3}$. The fitting function is $\log J = 17.5 \ln S/(T_c/T - 1)^{1.3} - 51$. This linear, empirical scaling relation seems to work well over a surprisingly wide range of nucleation rates, $J = (10^{-30} - 10^{-5})\sigma^{-3}\tau^{-1}$ for the MD data and the NPC (Nucleation Pulse Chamber) experiment¹⁴, but not for the MC simulations. Interestingly, a different scaling relation, $\ln S/(T_c/T - 1)^{3/2}$ has been found from experimental nucleation rates for several different substances such as water⁴¹, toluene⁶, and nonane⁷. Our results suggests the scaling relation depends on the substance type.

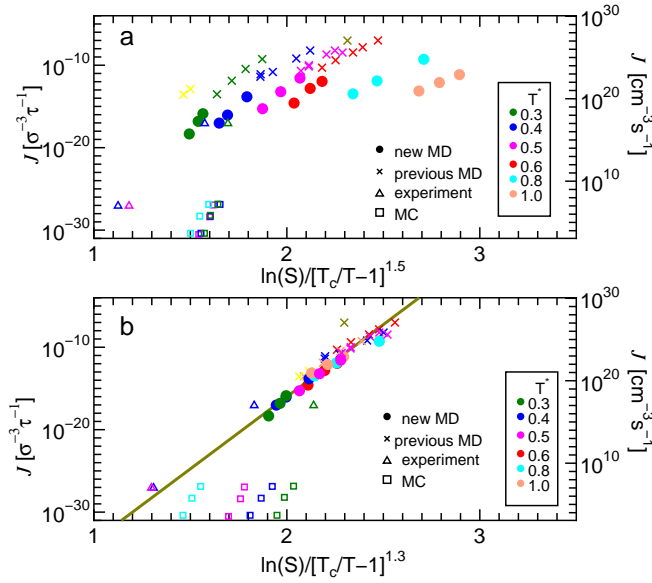


FIG. 1. Nucleation rates obtained by the MD simulations with LJ molecules and the experimental results for argon as a function of (a) $\ln S/(T_c/T - 1)^{1.5}$ and (b) $\ln S/(T_c/T - 1)^{1.3}$. The results for various supersaturation ratios S and temperatures T^* ($= kT/\epsilon$ in the Boltzmann constant k and the depth of the LJ potential ϵ) obtained by the large-scale MD simulations³⁷ and the previous ones^{16,31,36} are shown by the filled circles and the crosses, respectively. The results for MC simulations⁴² are shown with square markers, where the temperatures are $T^* = 0.7, 0.5, 0.419$, and 0.335 . The triangles show the experimental results for argon^{14,15}. We adopt $T_c = 1.312\epsilon/k$ (or 151 K) in the simulations (or experiments). In (b) the fitting function (solid line) for J [$\sigma^{-3}\tau^{-1}$] is given by $\log J = 17.5 \ln S/(T_c/T - 1)^{1.3} - 51$.

However, linear empirical scaling relations contradict one of the most basic, general expectations from nucleation theory: according to the nucleation theorem, the size of the critical cluster i^* is determined by the derivative $d(\ln J)/d(\ln S)$ ^{37,43}. These empirical scalings therefore imply a constant critical cluster size i^* at each temperature over a wide range in J . The corresponding free energy functions would need to peak at exactly the same size over a wide range in S and J , which seems impossible to achieve with any reasonably smooth surface energy function. Instead of a linear relation, one would instead expect some downward curvature in Fig. 1, which is consistent with the MD data points alone, but not in combination with the NPC experiment.

III. RECONSTRUCTING THE FORMATION FREE ENERGY FROM MD SIMULATIONS

We now derive the free energies of cluster formation directly from MD results and compare them with predictions from three widely used models: In the (modified) classical nucleation theory CNT (or MCNT) and in the

semi-phenomenological (SP) model^{8,11}, the free energies ΔG_i are respectively

$$\frac{\Delta G_{i,\text{CNT}}}{kT} = -i \ln S + \eta i^{2/3}, \quad (1)$$

$$\frac{\Delta G_{i,\text{MCNT}}}{kT} = -(i-1) \ln S + \eta(i^{2/3} - 1), \quad \text{and} \quad (2)$$

$$\frac{\Delta G_{i,\text{SP}}}{kT} = -(i-1) \ln S + \eta(i^{2/3} - 1) + \xi(i^{1/3} - 1) \quad (3)$$

where $S = P_1/P_e$ is the supersaturation ratio of monomers using the saturated vapor pressure P_e and the partial pressure of monomers P_1 , η and ξ are temperature-dependent quantities which can be fixed from the condensed phase surface tension, bulk density and the second virial coefficient^{8,37}. Note that the CNT assumes large cluster sizes, it is not expected to work for small clusters and its ΔG_i does not vanish at $i = 1$, i.e., for monomers.

The formation free energy of a cluster is directly related to the equilibrium size distribution $n_e(i)$:

$$\frac{\Delta G_i}{kT} = \ln \left(\frac{n(1)}{n_e(i)} \right), \quad (4)$$

where $n(1)$ is the number density of the monomers^{31,36,37}. For small subcritical clusters ($i \lesssim i^*$), the steady state size distribution $n(i)$, which can be measured in MD simulations, agrees very well with the equilibrium size distribution $n_e(i)$ ¹⁶, which lets us obtain ΔG_i for small clusters^{16,30,36-38}. Obtaining the *full* free energy landscape, including the crucial region around the critical sizes, requires a more sophisticated method, which takes the difference between steady state and equilibrium size distributions into account. A first procedure of this kind was proposed by Wedekind and Reguera⁴⁴ based on mean first passage time (MFPT) method. In principle it allows a full reconstruction based on a large number of small simulations, each one is run until it produces one nucleation event. However, the observation of one event does not demonstrate that the simulations are really sampling the assumed steady state nucleation regime, the passage times might include some initial lag time and a significant transient nucleation phase, which precedes the steady state regime⁴⁵. Both time-scales become quite large for LJ vapor-to-liquid nucleation at low temperatures³⁷.

Our recent, very large scale nucleation simulations allow very precise measurements of the cluster size distribution during a clearly resolved steady state nucleation regime and under realistic constant external conditions³⁷. Here we present a new method to obtain the full free energy landscape from these steady state size distributions: The nucleation rate is the net number of the transition from i -mers to $i+1$ -mers and given by

$$J = R^+(i)n(i) - R^-(i+1)n(i+1), \quad (5)$$

where $R^+(i)$ is the transition rate from a cluster of i molecules, i -mer, to $(i+1)$ -mer per unit time, i.e., the accretion rate, and $R^-(i)$ is the transition rate from i -mer to $(i-1)$ -mer per unit time, i.e., the evaporation rate

of i -mer. $R^+(i)$ is given by $R^+(i) = \alpha n(1)v_{\text{th}}(4\pi r_0^2 i^{2/3})$, where α is the sticking probability, v_{th} is the thermal velocity, $\sqrt{kT/2\pi m}$, and r_0 is the radius of a monomer, $(3m/4\pi\rho_m)^{1/3}$ where m is the mass of a molecule and ρ_m is the bulk density. The evaporation rate is obtained from the principle of detailed balance in thermal equilibrium:

$$R^-(i+1)n_e(i+1) = R^+(i)n_e(i). \quad (6)$$

From Eqs.(5) and (6), the nucleation rate is given by

$$J = \left[\sum_{i=1}^{\infty} \frac{1}{R^+(i)n_e(i)} \right]^{-1} \simeq R^+(i_*)n_e(i_*)Z, \quad (7)$$

with the Zeldovich factor, Z .

From Eqs.(5) and (6), we obtain

$$\frac{n_e(i)}{n(i)} = \frac{n_e(i-1)}{n(i-1)} \left(1 - \frac{J}{R^+(i-1)n(i-1)} \right)^{-1}. \quad (8)$$

Equation (8) is a recurrence relation and enables us to obtain $n_e(i)$ if $J, n(i)$ and $n_e(i-1)$ are known³⁸. Fig. 2 shows $n_e(i)$, $n(i)$, and $\Delta G_i(S)$ derived by Eq. (8) for a typical example ($T^* = kT/\epsilon = 0.6$ and $S = 16.9$ which corresponds to the case T6n80 in Table III in Diemand et al.³⁷). $\Delta G_i(S=1)$ is a surface term corresponding to the work required to form the vapor-liquid interface. From Eq. (8), we obtain $\Delta G_i(S=1)$:

$$\Delta G_i(S=1) = \Delta G_i(S) + (i-1) \ln S, \quad (9)$$

using the dependence of the supersaturation in the theories except the CNT. Fig. 2 also shows $\Delta G_i(S=1)$.

The surface terms of free energy $\Delta G_i(S=1)$ at various temperatures and supersaturation ratios obtained by MD simulations are shown in Figure 3, where we evaluated $R^+(i)$ using α obtained by the MD simulations (Table III in Diemand et al.). From Figure 3, we confirm $\Delta G_i(S=1)$ depends only on temperature, which implies that the volume term in Eqs.(2) and (3) works very well.

The peaks of the free energy curves give critical cluster sizes which agree very well with those from the nucleation theorem (see Fig. 7). Since the nucleation rates, which enter into the nucleation theorem, do not depend on the detailed cluster definition, this good agreement provides a robust confirmation, that the simple Stillinger criterion used here^{36,37} gives realistic cluster size estimates. An earlier study³¹ found that critical sizes based on the Stillinger definition are up to a factor 2 larger than independent estimates from the nucleation theorem. This contradiction can be resolved by a detailed comparison with other MD simulations at very similar conditions³⁶: Using the initial supersaturations S_0 in the nucleation theorem (as in³¹) instead of the actual supersaturation S during the simulation³⁶, leads one to underestimate the critical sizes by up to a factor of 1.8, which eliminates the discrepancy reported in³¹.

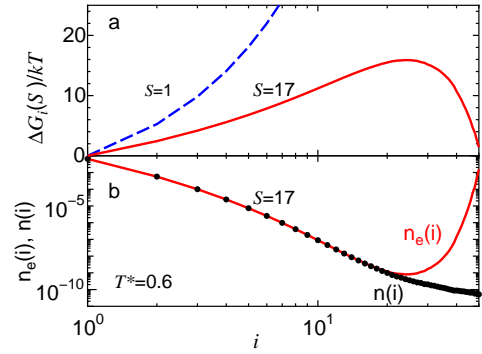


FIG. 2. (a) $\Delta G_i(S)/(kT)$ as a function of i , where $T^* = kT/\epsilon = 0.6$ and $S = 16.9$ (T6n80 in Table III in Diemand et al.³⁷). The dashed line shows $\Delta G_i(S)/(kT)$ at $S = 1$. (b) The equilibrium number density of i -mers $n_e(i)$ [σ^{-3}] (solid curve) and the steady number density obtained by the simulation $n(i)$ [σ^{-3}] (circles).

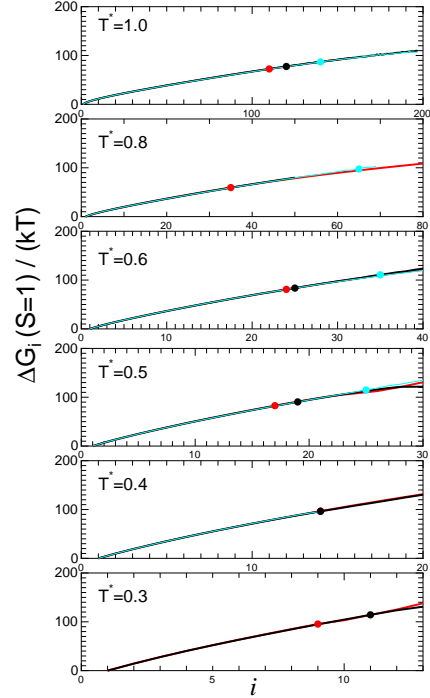


FIG. 3. $\Delta G_i(S=1)$ as a function of i for various temperatures. At each temperature, we show $\Delta G_i(S=1)$ obtained by the different values of the supersaturation ratio. The circles show the critical clusters derived by the maximum of $\Delta G_i(S)$ for various supersaturation ratios S . We can confirm $\Delta G_i(S=1)$ depends on only T .

IV. A NEW SCALING FOR NUCLEATION RATES

Fig. 4 shows the surface energy $\Delta G_i(S=1)$ divided by that of the CNT, $\Delta G_i(S=1)/(\eta i^{2/3} kT)$, as a function of $i^{-1/3}$. The theoretical evaluations are also shown in Fig. 4. The simulation results agree with the SP model at $0.5 \lesssim i^{-1/3} < 1$, but deviate from the model

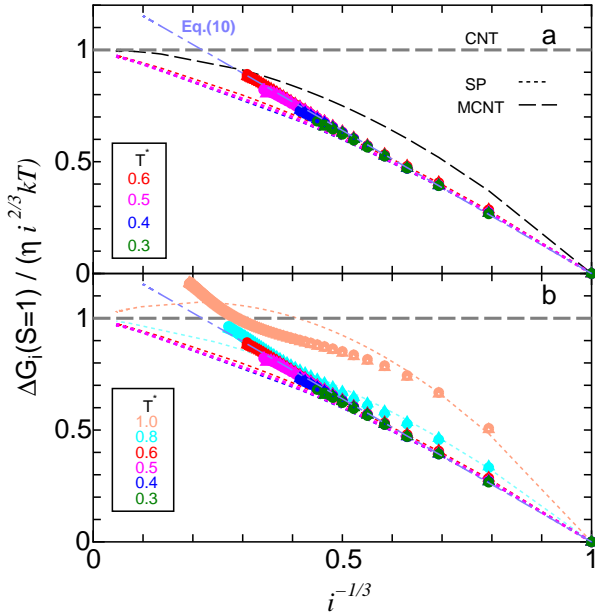


FIG. 4. (a) $\Delta G_i(S=1)/(\eta i^{2/3}kT)$ as a function of $i^{-1/3}$ at $kT/\epsilon \leq 0.6$. Results obtained from 11 MD simulations are plotted with symbols: different symbols indicate the MD results starting from different supersaturation ratios. We find that they are universal, which implies that $\Delta G_i(S=1)/(\eta i^{2/3}kT)$ is independent of temperature for ($T \leq 0.6$). From the fitting, we obtain $\Delta G_i(S=1)/(\eta i^{2/3}kT) = 1.28(1 - i^{-1/3})$ (the dotted-dashed line). The results by the SP (dotted lines) and MCNT (dashed line) are also shown. $\Delta G_i(S=1)/(\eta i^{2/3}kT) = 1$ in the CNT. (b) The same as (a) but for all temperatures.

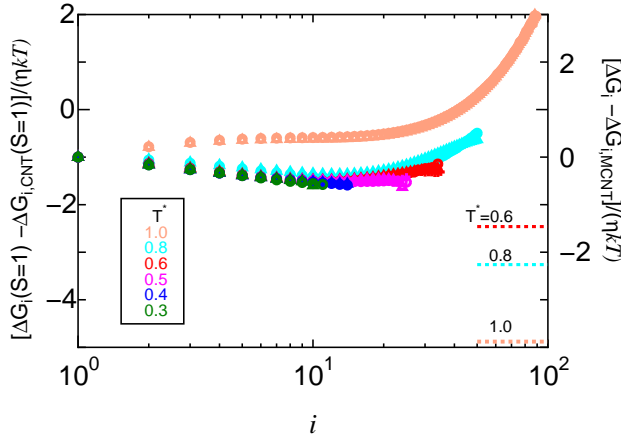


FIG. 5. The difference in $\Delta G_i(S=1)$ between MD results and the CNT divided by ηkT , $[\Delta G_i(S=1) - \Delta G_{i,\text{CNT}}(S=1)]/(\eta kT)$ as a function of i at various temperatures. Different symbols indicate the MD results starting from different supersaturation ratios. The results of McGraw and Laaksonen⁴⁷ are also shown by dotted lines for $T^* = 0.6, 0.8$ and 1.0 . The right vertical axis shows the value of the difference between the MD results and the MCNT, $[\Delta G_i - \Delta G_{i,\text{MCNT}}]/(\eta kT)$, which is valid for any value of S .

for larger clusters of $i^{-1/3} < 0.5$. Surprisingly, $\Delta G_i(S=1)/(\eta i^{2/3}kT)$ is almost the same for all results obtained by 11 MD simulations for temperatures below the triple point. This indicates that $\Delta G_i(S=1)/(\eta i^{2/3}kT)$ is a function of i and independent of the temperature. From the fitting of the results, we obtain

$$\frac{\Delta G_i(S=1)}{\eta i^{2/3}kT} = f(i) = A(1 - i^{-1/3}), \quad (10)$$

where $A = 1.28$. The fitting function is also shown by the dotted-dashed line in Fig. 4. Equation (10) implies a constant, positive Tolman length of $\delta = 0.5r_0$ and the constant A sets an effective normalisation factor for the planar surface energy (or the surface area), if we interpret $\Delta G_i(S=1)/(\eta i^{2/3}kT) = a_i \gamma_i / (4\pi r_0^2 \gamma)$, where $\gamma_i = \gamma[1 - 2\delta/(r_0 i^{1/3})]$ and a_i are the surface tension and surface area of the cluster and γ is the planar surface tension. Equation (10) could be a promising candidate for an accurate nucleation theory, in which A is temperature independent below the triple point. Our result indicates that at low temperatures the Tolman relation is valid even for very small clusters including 2-30 atoms.

McGraw and Laaksonen^{46,47} obtained ΔG_i of large clusters ($i \gtrsim 50$) with density functional calculations. They found that the deviation of ΔG_i from the CNT is temperature dependent, but independent of the cluster size. Figure 5 shows the difference of $\Delta G_i(S=1)$ between MD results and the CNT, *i.e.*, $\Delta G_i(S=1) - \Delta G_{i,\text{CNT}}(S=1)$ as a function of i . We find these differences are nearly constant around $i \sim 10$ for each temperature. But they increase with the size for $i > 20$. According to McGraw and Laaksonen (1997)⁴⁷, on the other hand, $[\Delta G_i(S=1) - \Delta G_{i,\text{CNT}}(S=1)]/(\eta kT)$ are calculated to be -2.46, -3.26, and -4.88 for $T^* = 0.6, 0.8$, and 1.0 , respectively.

Using Eq. (10), the critical cluster i_* is obtained by

$$i_* = \left(\frac{A\eta}{3 \ln S} \right)^3 \left(1 + \sqrt{1 - \frac{3 \ln S}{A \eta}} \right)^3, \quad (11)$$

from the following relation

$$-\frac{\ln S}{\eta} + \frac{2}{3} i_*^{-1/3} f(i_*) + i_*^{2/3} f'(i_*) = 0, \quad (12)$$

where we have assumed that the molecular volume is far smaller in the liquid phase than in the gas phase. The detailed derivation is given in the Appendix.

We also derive the analytical formula for the nucleation rate:

$$\ln J' = \ln[\alpha Z i_*^{2/3}] + (i_* + 1) \ln S - i_*^{2/3} \eta f(i_*), \quad (13)$$

where J' is a dimensionless nucleation rate defined by $J' = J/(4\pi r_0^2 n_{\text{sat}}^2 v_{\text{th}})$ with the saturated number density of monomers $n_{\text{sat}} (= n(1)/S)$ and the Zeldvich factor is given by

$$Z = \frac{1}{3} i_*^{-2/3} \sqrt{\frac{A\eta}{\pi} (1 - i_*^{-1/3})}. \quad (14)$$

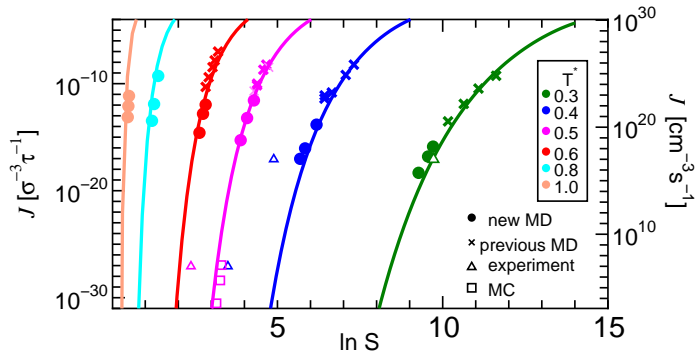


FIG. 6. The nucleation rate as a function of the supersaturation ratio. The analytical formula for the nucleation rates are shown by solid lines. The results for various temperature and supersaturation ratios by the large-scale MD simulations³⁷ and the previous ones^{31,36} are shown by the filled circles and the crosses, respectively. The results for MC simulations⁴² are shown by the squares, where the temperature is $T^* = 0.5$. The triangles show the experimental results for argon^{14,15}.

Fig. 6 shows the nucleation rate as a function of $\ln S$ obtained by the MD simulations and the analytical formula. We find good agreements between the analyses and the simulations for the various temperatures and supersaturation ratios.

Our finding that $\Delta G_i(S=1)/(\eta i^{2/3}kT)$ is independent of the temperature leads to a scaling relation. Equation (12) indicates that i_* is a function of only $\ln S/\eta$. Thus from Eq. (13) $\ln J'/\eta$ is determined only by $\ln S/\eta$, neglecting a term including Zeldovich factor which is smaller than the other terms. Fig. 7 shows the size of critical clusters and $\ln J'/\eta$ obtained by MD and MC simulations and experiments as a function of $\ln S/\eta$. We confirm that $\ln J'/\eta$ is scaled by $\ln S/\eta$ almost perfectly for MD simulations, at $T^* \leq 0.6$. At high temperatures ($T^* > 0.8$), $\ln J'/\eta$ deviates from the scaling relation. This would come from the deviation of $f(i)$, i.e., $f(i)$ depends on T at $T^* > 0.8$ (see Fig. 4(b)). Fig. 7 shows this scaling also works for one SNN experiment ($T^* = 0.3$) and the MC simulations at $T^* = 0.5$ and 0.7 , although some MC data and experiments deviate from the scaling relation.

V. SUMMARY AND CONCLUSIONS

We derived for the first time the formation free energy of a cluster over a wide range of cluster sizes and temperatures from recent very large-scale MD simulations. The peaks of the free energy curves give critical cluster sizes, which agree well with independent estimates based on the nucleation theorem. This implies that the simple Stillinger criterion used here gives realistic cluster size estimates.

At low temperatures the free energies show a universal deviation from the CNT, which allows us to derive a

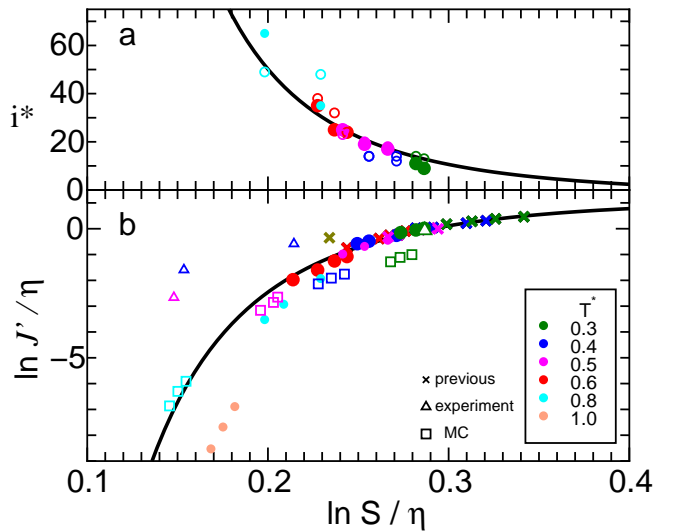


FIG. 7. We propose that (a) the size of critical cluster and (b) $\ln J'/\eta$ are determined only by $\ln S/\eta$, where $J' = J/(4\pi r_0^2 n_{\text{sat}}^2 v_{\text{th}})$. The analytical formula obtained by our model are shown by the solid lines. Panel (a) shows, that the critical clusters sizes derived from the maximum of $\Delta G_i(S)$ (filled circles) and from the nucleation theorem (open circles, i_{NT} in Diemand et al.³⁷) agree very well with each other and also with our analytical model. In (b), the results for various temperature and supersaturation ratios by the large-scale MD simulations³⁷ and the previous ones^{16,31,36} are shown by the filled circles and the crosses, respectively. The results for MC simulations⁴² are shown with square markers. The triangles show the experimental results for argon^{14,15}.

new scaling relation for nucleation: $\ln J'/\eta$ is scaled by $\ln S/\eta$. This scaling relation predicts the critical cluster size very well. The relation can be explained from a surface energy required to form the vapor-liquid interface and implies a constant, positive Tolman length of $\delta = 0.5r_0$. Generally, $\Delta G_i(S=1)$ is written as the surface energy multiplied by the surface area, $a_i\gamma_i$. In the theory, the cluster is always assumed to be spherical and has the same density as the bulk liquid. However, our analyses of cluster properties show larger surface areas (Angéilil et al.⁴⁸). The higher normalisation ($A \simeq 1.28$ in Eq. (10)) of $\Delta G_i(S)$ relative to the models might be caused by these larger surface areas. The scaling relation and the relation between the cluster properties and ΔG_i should be investigated in more detail for various materials.

VI. ACKNOWLEDGMENTS

We thank the anonymous reviewers for their valuable suggestions which have improved the quality of the paper. This work was supported by the Japan Society for the Promotion of Science (JSPS). J.D. and R.A. acknowledge support from the Swiss National Science Foundation (SNSF).

VII. APPENDIX

The general expression for the minimum work $\Delta G(r)$ required to form a cluster of radius r , is given by⁴⁹

$$\Delta G(r) = \frac{V_1}{v_l} [\mu_l(P_l) - \mu_g(P_g)] - (P_l - P_g)V_1 + a_i \gamma_i \quad (15)$$

where μ_l and μ_g are the chemical potentials of liquid and gas, P_l and P_g are the pressures of metastable liquid and gas, and v_l and $V_1 (= i v_l = 4\pi r^3/3)$ are the molecular volumes of liquid and the volumes of a cluster respectively. Using $\mu_l(P_e) = \mu_g(P_e)$ and $\mu_l(P_l) - \mu_l(P_e) = v_l(P_l - P_e)$, we obtain

$$\begin{aligned} \Delta G(r) &= \frac{V_1}{v_l} [\mu_g(P_e) + v_l(P_l - P_e) - \mu_g(P_g)] \\ &\quad - (P_l - P_g)V_1 + a_i \gamma_i, \\ &= \frac{V_1}{v_l} [\mu_g(P_e) - \mu_g(P_g)] + (P_g - P_e)V_1 + a_i \gamma_i, \\ &= \frac{V_1}{v_l} [\mu_g(P_e) - \mu_g(P_g)] + i(S-1)kT \frac{v_l}{v_g} + a_i \gamma_i, \end{aligned} \quad (16)$$

where v_g is the molecular volume in the gas phase. For the case $v_l \ll v_g$, the second term on the right hand side of Eq. (16) is negligible. Assuming $a_i \gamma_i = 4\pi r^2 \gamma$, we obtain the formula for the critical radius r_{cr} called the Kelvin relation⁵⁰ from $\partial \Delta G(r)/\partial r = 0$:

$$r_{cr} = \frac{2\gamma v_l}{\Delta\mu}, \quad (17)$$

where $\Delta\mu = \mu(P_g) - \mu_g(P_e) = kT \ln S$.

From Eq. (10), the result from MD simulations shows

$$a_i \gamma_i = 4\pi r^2 A \gamma (1 - r_0/r), \quad (18)$$

thus we obtain the following relation at $r = r_{cr}$:

$$- \frac{4\pi r_{cr}^2 \Delta\mu}{v_l} + 8\pi r_{cr} A \gamma - 4\pi r_0 A \gamma = 0. \quad (19)$$

From Eq. (19), r_{cr} is given by

$$r_{cr} = \frac{A\gamma v_l}{\Delta\mu} \left(1 + \sqrt{1 - \frac{\Delta\mu r_0}{v_l A \gamma}} \right), \quad (20)$$

which corresponds to Eq. (11).

¹M. Volmer and A. Weber, Z. Phys. Chem. **119**, 277 (1926).

²V. R. Becker and W. Döring, Ann. Phys. **416**, 719 (1935).

³J. Feder, K. C. Russell, J. Lothe, and G. M. Pound, Adv. Phys. **15**, 111 (1966).

⁴R. J. Anderson, R. C. Miller, J. L. Kassner, and D. E. Hagen, J. Atmos. Sci. **37**, 2508 (1980).

⁵J. L. Schmitt, G. W. Adams, and R. A. Zalabsky, J. Chem. Phys. **77**, 2089 (1982).

⁶J. L. Schmitt, R. A. Zalabsky, and G. W. Adams, J. Chem. Phys. **79**, 4496 (1983).

⁷G. W. Adams, J. L. Schmitt, and R. A. Zalabsky, J. Chem. Phys. **81**, 5074 (1984).

⁸A. Dillman and G. E. A. Meier, J. Chem. Phys. **94**, 3872 (1991).

⁹D. W. Oxtoby, J. Phys.: Condens. Matter **4**, 7627 (1992).

¹⁰Y. Viisanen, R. Strey, and H. Reiss, J. Chem. Phys. **99**, 4680 (1993).

¹¹A. Laaksonen, I. J. Ford, and M. Kulmala, Phys. Rev. E **49**, 5517 (1994).

¹²Y. Viisanen and R. Strey, J. Chem. Phys. **101**, 7835 (1994).

¹³K. Hämeri and M. Kulmala, J. Chem. Phys. **105**, 7696 (1996).

¹⁴K. Iland, J. Wölk, R. Strey, and D. Kashchiev, J. Chem. Phys. **127**, 154506 (2007).

¹⁵S. Sinha, A. Bhabhe, H. Laksmono, J. Wölk, R. Strey, and B. Wyslouzil, J. Chem. Phys. **132**, 064304 (2010).

¹⁶K. Yasuoka and M. Matsumoto, J. Chem. Phys. **109**, 8451 (1998).

¹⁷K. Yasuoka and M. Matsumoto, J. Chem. Phys. **109**, 8463 (1998).

¹⁸P. R. ten Wolde and D. Frenkel, J. Chem. Phys. **109**, 9901 (1998).

¹⁹K. J. Oh and X. C. Zeng, J. Chem. Phys. **110**, 4471 (1999).

²⁰B. Senger, P. Schaaf, D. S. Corti, R. Bowles, D. Pointu, J.-C. Voegel, and H. Reiss, J. Chem. Phys. **110**, 6438 (1999).

²¹P. R. ten Wolde, M. J. Ruiz-Montero, and D. Frenkel, J. Chem. Phys. **110**, 1591 (1999).

²²K. Laasonen, S. Wonczak, R. Strey, and A. Laaksonen, J. Chem. Phys. **113**, 9741 (2000).

²³K. J. Oh and X. C. Zeng, J. Chem. Phys. **112**, 294 (2000).

²⁴H. Vehkamäki and I. J. Ford, J. Chem. Phys. **112**, 4193 (2000).

²⁵B. Chen, J. I. Siepmann, K. J. Oh, and M. L. Klein, J. Chem. Phys. **115**, 10903 (2001).

²⁶P. Schaaf, B. Senger, J.-C. Voegel, R. K. Bowles, and H. Reiss, J. Chem. Phys. **114**, 8091 (2001).

²⁷J. Wölk and R. Strey, J. Phys. Chem. B **105**, 11683, (2001).

²⁸J. Merikanto, H. Vehkamäki, and E. Zapadinsky, J. Chem. Phys. **121**, 914 (2004).

²⁹K. K. Tanaka, K. Kawamura, H. Tanaka, and K. Nakazawa, J. Chem. Phys. **122**, 184514 (2005).

³⁰H. Matsubara, T. Koishi, T. Ebisuzaki, and K. Yasuoka, J. Chem. Phys. **127**, 214507 (2007).

³¹J. Wedekind, J. Wölk, D. Reguera, and R. Strey, J. Chem. Phys. **127**, 154515 (2007).

³²M. Horsch, J. Vrabec, and H. Hasse, Phys. Rev. E **78**, 011603 (2008).

³³M. Horsch, and J. Vrabec, J. Chem. Phys. **131**, 184104 (2009).

³⁴J. Wedekind, G. Chkonia, J. Wölk, R. Strey, and D. Reguera, J. Chem. Phys. **131**, 114506 (2009).

³⁵I. Napari, J. Julin, and H. Vehkamäki, J. Chem. Phys. **133**, 154503 (2010).

³⁶K. K. Tanaka, H. Tanaka, T. Yamamoto, and K. Kawamura, J. Chem. Phys. **134**, 204313, (2011).

³⁷J. Diemand, R. Angéilil, K. K. Tanaka, and H. Tanaka, J. Chem. Phys. **139**, 074309. (2013).

³⁸K. K. Tanaka, A. Kawano, and H. Tanaka, J. Chem. Phys. **140**, 114302 (2014).

³⁹B. N. Hale, Phys. Rev. A **33**, 4156 (1986).

⁴⁰B. N. Hale, Metall. Trans. A **23A**, 1863 (1992).

⁴¹B. N. Hale, J. Chem. Phys. **122**, 204509 (2005).

⁴²B. N. Hale and M. Thomason, Phys. Rev. Lett. **105**, 046101 (2010).

⁴³V. I. Kalikmanov, *Nucleation theory*, Lecture notes in Physics (Springer, Dordrecht, 2013), Vol. 860.

⁴⁴J. Wedekind and D. Reguera, J. Phys. Chem. B **112**, 11060 (2008).

⁴⁵V. Shneidman, K. Jackson, and K. Beatty, Phys. Rev. B **59**, 3579 (1999)

⁴⁶R. McGraw and A. Laaksonen, Phys. Rev. Lett. **76**, 2754 (1996).

⁴⁷R. McGraw and A. Laaksonen, J. Chem. Phys. **106**, 5284 (1997).

⁴⁸R. Angéilil, J. Diemand, K. K. Tanaka, and H. Tanaka, J. Chem. Phys. **140**, 074303 (2014).

⁴⁹L. D. Landau and E. M. Lifshitz, *Statistical Physics* (Pergamon press, Oxford, 1980), section 162.

⁵⁰A. Laaksonen and R. McGraw, Europhys. Lett. **35**, 367 (1996).